Reinforced Thermoplastic Polyimide with Dispersed Functionalized Single Wall Carbon Nanotubes

Marisabel Lebrón-Colón,*,† Michael A. Meador,† James R. Gaier,† Francisco Solá,† Daniel A. Scheiman,‡ and Linda S. McCorkle§

NASA Glenn Research Center, 21000 Brookpark Road, Cleveland, Ohio 44135, and Ohio Aerospace Institute, 22800 Cedar Point Road, Brookpark, Ohio 44142

ABSTRACT Molecular π-complexes were formed from pristine HiPCO single- wall carbon nanotubes (SWCNTs) and 1-pyrene- *N*-(4-*N*′-(5-norbornene-2,3-dicarboxyimido)phenyl butanamide, **1**. Polyimide films were prepared with these complexes as well as uncomplexed SWCNTs and the effects of nanoadditive addition on mechanical, thermal, and electrical properties of these films were evaluated. Although these properties were enhanced by both nanoadditives, larger increases in tensile strength and thermal and electrical conductivities were obtained when the SWCNT/**1** complexes were used. At a loading level of 5.5 wt %, the T_g of the polyimide increased from 169 to 197 °C and the storage modulus increased 20-fold (from 142 to 3045 MPa). The addition of 3.5 wt % SWCNT/**1** complexes increased the tensile strength of the polyimide from 61.4 to 129 MPa; higher loading levels led to embrittlement and lower tensile strengths. The electrical conductivities (DC surface) of the polyimides increased to 1×10^{-4} Scm^{-1} (SWCNT/**1** complexes loading level of 9 wt %). Details of the preparation of these complexes and their effects on polyimide film properties are discussed.

KEYWORDS: single-wall carbon nanotubes • polymer nanocomposites • thermoplastic polyimide • aromatic functionalization • electron microscopy

1. INTRODUCTION

A number of theoretical (1–7) and experimental (8–10) studies confirm that single-wall carbon nanotubes (SWCNTs) possess extraordinary mechanical, electrical, and chemical properties. Their excellent strength, stiffness, stability, and high conductivity (both thermal and electrical) are due to the perfect alignment of the carbon atomic lattice along the tube axis and their closed topology (11). The extraordinary properties observed in SWCNTs offer advantages over many conventional reinforcement materials (e.g., carbon fibers), not only because they have superior properties but also because SWCNTs have a large surface area (i.e., 285 m^2/g for SWCNTs ropes; the total outer surface area of the individual tubes is about 1300 m^2/g), which could be very useful for structural and chemical applications (11, 12). The intrinsic properties of SWCNTs make them ideal materials for potential use in aeronautics and space exploration missions. Their high modulus (100 times that of steel at one-sixth of the density) and low weight make SWCNTs ideal reinforcements in ultra lightweight, high strength, and stiffness composite materials for use in large-area antennas, solar arrays, solar sails, and radiation shielding materials for vehicles, habitats, and space suits. In addition, the ability to enhance thermal and electrical conductivity as well as mechanical properties opens the possibility of utilizing SWCNTs in the development of multifunctional materials, e.g., structural composites with enhanced electrical conductivity for lightning strike protection of aircraft.

A variety of polymers (13–18) including epoxies (19–24) have been used to prepare carbon nanotube (CNTs) polymer nanocomposites with the aim of obtaining enhanced mechanical, thermal, and electrical properties. These studies agree that an important requirement for the effective use of single wall or multiwall carbon nanotubes as reinforcements is the ability to homogenously disperse the nanotubes into the polymeric material. Homogeneous dispersion of carbon nanotubes throughout the polymeric resins will lead to efficient load transfer, which is necessary for the desired improvement in mechanical properties and will also produce nanocomposite with optimum electrical conductivity. However, dispersion of single-wall carbon nanotubes in a polymeric material and the development of strong matrix−nanotube bonding are confounded by the insolubility of SWCNTs in organic solvents and by their tendency to agglomerate because of strong Van der Walls interactions. Functionalization of SWCNTs can overcome these issues.

Covalent (25–33) and noncovalent (34–55) functionalization of CNTs has been demonstrated to improve their dispersibility in various polymer matrices and enhance interfacial bonding between the polymer and the carbon nanotubes. Covalent functionalization techniques have been successful in the production of high-quality nanocomposites. However, these methods often involve the conversion of

* Corresponding author. Tel.: (216) 433 2292. Fax: (216) 977 7132. E-mail: Marisabel.lebron-colon-1@nasa.gov.
Received for review October 7, 2009 and accepted February 3, 2010
† NASA Glenn Research Center.
‡ Employed by ASRC, Cleveland, OH 44135.
§ Ohio Aerospace Institute.
DOI: 10.1021/am900682s

side-wall carbons from sp^2 to sp^3 hybrization. This bonding change disrupts conjugation within the nanotubes and can lead to reduced electrical conductivity and mechanical properties. Accordingly, noncovalent methods such as wrapping or complexation have been explored as an alternative to the covalent functionalization methods described above. Such methods lead to enhanced solubility and good carbon nanotubes polymer interactions with no adverse effect on carbon nanotube properties.

Noncovalent functionalization of carbon nanotubes using highly aromatics molecules have been proved to be very effective (48–55). It has been demonstrated that pyrene interact strongly on the surface wall of either single (48) or multiwall carbon nanotubes (55). The interaction between the pyrene and the carbon nanotubes was proof to be very efficient for the immobilization of proteins and bimolecules (48). Other molecules that have been reported to formed effective interaction with the carbon nanotubes sidewalls include conjugated aromatic diazo dye and fluorescein-polyethylene glycol, polycyclic aromatic anthracenes, and heterocyclic aromatic porphyrins and phthalocyanins. All these reports show that indeed interaction via π-stacking occur between the aromatic molecules and the carbon nanotubes surfaces inducing the nanotubes to disperse better and for longer period of time in organic solvents. Among the polycyclic molecules, pyrene has been mostly used because it forms the stronger π-stacking interaction with carbon nanotubes.

Although in the literature can be found a number of examples of noncovalent functionalized SWCNTs, the methods reported to be more used to investigate the effect on mechanical, thermal, and/or electrical properties of polymeric nanocomposites include the use of sodium dodecyl sulfate, sodium dodecylbenzene sulfonate, DNA, and conjugated polymers that tend to wrap the nanotubes (34–45). To the best of our knowledge, noncovalent functionalized SWCNTs with norbornene end-capped pyrene butanamide **1** have not been used in polyimide nanocomposite films. Thus, that motivates us to prepare these molecular complexes between the SWCNTs to study their effect on mechanical, thermal, and electrical properties in polyimide matrix. Herein we present the preparation of the complexes and uncomplexed SWCNTs used in polyimide nanocomposite films and a comparison of the loading effects of these on the mechanical, thermal and electrical properties of these films.

2. EXPERIMENTAL SECTION

2.1. Materials. Unpurified single-walled carbon nanotubes (SWCNTs) obtained for this study were synthesized at Rice University using the high pressure CO disproportionate (HiPCO) process developed by Smalley et al. (56). The SWCNTs were purified in gram quantities by a modified heat/oxidative technique that reduce the iron content of HiPCO SWCNTs to less than 0.05 wt % (57, 58).

All reagents and solvents were purchased from commercial sources as identified and used without further purification. *o*-Chlorobenzene (OCB), dichloromethane (CH_2Cl_2), chloroform ($CHCl_3$), tetrahydrofuran (THF), dimethylformamide (DMF), *N*-methyl-2-pyrrolidone (NMP), methanol (MeOH), ethanol (EtOH), thionyl chloride ($SOCl_2$), triethylamine (Et_3N), sodium carbonate (Na_2CO_3), and sodium sulfate (Na_2SO_4) were purchased from Sigma-Aldrich. Hydrochloric acid (HCl) and nitric acid (HNO_3) were purchased from Fisher. The 1-pyrenebutanoic acid used in this study was purchased from both Molecular Probes Inc. and Sigma-Aldrich. 2,2-Bis[4-(4-aminophenoxy)phenyl] propane (BAPP) was purchased from the Wakayama-Seika-Kogyo Company. Bisphenol-A-dianhydride (BPADA) was purchased from GE Plastics.

2.2. Characterization. Thermal gravimetric analysis (TGA) was performed on a TA model 2950 hi-res thermal gravimetric analyzer. These analysis were conducted in either air or nitrogen atmosphere, as indicated, at a heating rate of 10 °C min^{-1}. One sample for each film was used to carry out the dynamic mechanical analysis (DMA) measurement performed on a TA Instruments model 2980. These analyses were used to determine the modulus and the glass transition temperature (T_g) of the nanocomposites. Each sample was run on multifrequency-tension film. Thermomechanical analysis (TMA) was performed on a TA Instruments model 2940 to determine the coefficient of thermal expansion (CTE) of the nanocomposites. Scanning Electron Microscopy (SEM) photomicrographs were recorded on a Hitachi model S-4700 field-emission scanning electron microscope using 10 kV beam energy. FT-IR spectra were measured in a KBr pellet using a Nicolet model 510p FT-IR spectrometer. Ultraviolet−visible (UV−vis) absorption spectra were recorded in solutions, solvent as indicated, with a Shimadzu model UV-3101PC spectrometer, using a 10 mm light path cell from Apple Scientific, Inc.

Mechanical properties were obtained with an Instron Model 4505 load frame using the series IX data acquisition software. At least six samples were measured for each film cut in a type V dog-bone specimen, in accordance with ASTM method D882.

Electrical resistivities were measured as follows: a sample of approximately 3.5 × 0.7 cm^2 specimens cut from the edge of each thermoplastic polyimide nanocomposite film toward the center. The thickness, width, and length dimensions were measured using a digital micrometer (note that the length is not the length of the sample, but the gauge length between the electrodes). The samples were mounted using spring clips into a Keithley model 8002 high resistance test box. No surface treatments were used to lower the contact resistance. A constant voltage of 100 V DC was applied across the sample using a Keithley model 247 high voltage supply. Current was monitored with a Keithley model 617 electrometer.

2.3. Synthesis. *1-Pyrene-(4-(N′-5-norbornene-2,3-dicarboximide)benzene) Butanamide,* 1. Butanamide **1** was prepared in two steps as shown in Scheme 1. A solution of 1-pyrenebutanoic acid (1.0 g, 3.47 mmol) in 5−10 mL of $CHCl_3$ was added to a 50 mL, three-necked, round-bottom flask equipped with a condenser and magnetic stirrer. Thionyl chloride (0.38 mL, 5.20 mmol, 1.5 equiv) was added to this suspension and the resulting mixture was refluxed for 2 h. (Note: longer reflux times tended to decrease the product yield.) The reaction solution was then cooled to room temperature and carefully transferred by pipet to a single neck round-bottom flask and the solvent and excess thionyl chloride was removed under vacuum. (The addition of a small amount of THF aided in the removal of excess $SOCl_2$.) The brownish-yellow 1-pyrene butanoylchloride was used directly in the next step without further purification. A solution of *N*-(4-aminophenyl)-5-norbornene-2,3-dicarboximide (0.53 g, 3.26 mmol) and Et_3N (0.45 mL, 3.23 mmol) in 5 mL of $CHCl_3$ was added under nitrogen to a two-neck, round-bottom flask equipped with a condenser. The reaction was cooled to 0 °C using an ice bath. A solution of crude 1-pyrenebutanoyl chloride in about 5 mL of $CHCl_3$ was carefully added and the reaction mixture was stirred overnight. The reaction mixture was then washed first with 5% HCl (2 × 25 mL), and then with a saturated

Scheme 1. Preparation of 1-Pyrene-(4-(*N*′-5-norbornene-2,3dicarboximide)benzene) Butanamide (1)

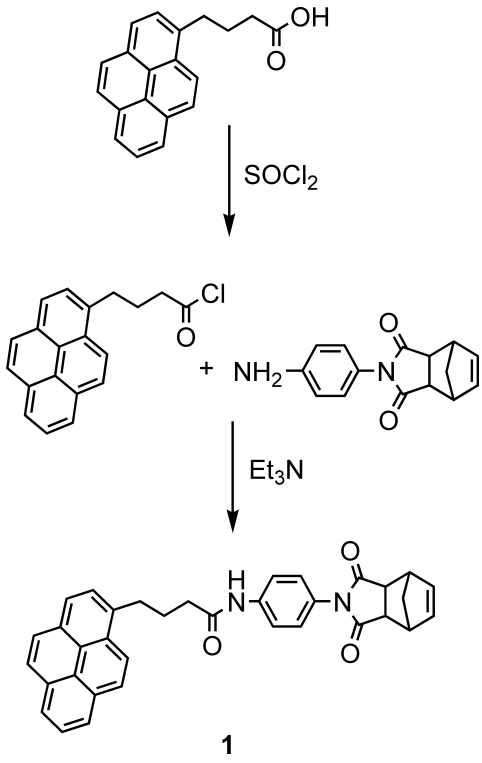

1

aqueous solution of Na_2CO_3 (1 × 10 mL). The organic phase was dried (Na_2SO_4), filtered, and concentrated under a vacuum. (Note: When the product is obtained as a "fluffy" solid, it is redissolved in a minimum amount of $CHCl_3$, transferred to a beaker, slowly air-dried, and then placed in a vacuum oven at ~65 °C to completely remove the solvent). The product was obtained as a yellow solid in typical reaction yields of about 65%. ^{1}H NMR (200 MHz, $CDCl_3$/TMS, δ): 1.38 (d, J = 23.8 Hz, 1H, −CH), 1.63 (d, J = 23.8 Hz, 1H, −CH), 2.04−2.31 (m, 4H, −CH), 3.20 (d, J = 67.6 Hz, 6H, $-CH_2$), 6.13 (s, 2H, HC=CH), 6.91 (d, J = 26.2 Hz, 2H, Ar−H), 7.41 (d, J = 29.0 Hz, 2H, Ar−H), 7.56−8.27 (m, 9H, Ar−H). FT-IR (KBr): NH (3341 cm^{-1}), CH (2943 cm^{-1}), CO (1704 cm^{-1}), aromatics (1500−1200 cm^{-1}).

SWCNT/1 Complexes. DMF (10 mL) was added to SWCNTs (0.050 g) and the resulting mixture was ultra sonicated for 30 min. A solution of pyrene derivative **1** (0.200 g, 0.38 mmol) in 10 mL of DMF was added and the mixture was placed in the refrigerator (0 °C) for 24 h. The suspension was then centrifuged for 30 min and the supernatant removed with a pipet leaving the SWCNT/**1** complexes in the bottom of the vial. The SWCNT/**1** complexes were washed with cold DMF (20 mL) until the presence of uncomplexed **1** could not be detected in the solvent (monitored by thin layer chromatography (TLC)). The solution was vigorously shaken and centrifuged (1400 rpm) each time. The complex was then washed with cold methanol (20 mL) the solution vigorously shaken, centrifuged for about 20 min, and the supernatant removed. The SWCNT/**1** complexes were dried in a vacuum oven at room temperature to a constant weight.

Polyimide (2). Polyimide **2** was prepared from BPADA and BAPP (Scheme 2). BPADA (10.0 g, 19.2 mmol), BAPP (7.88 g, 19.2 mmol) and anhydrous NMP (115 mL, 15 wt % solid) were added to a 250 mL round-bottom and condenser that had been flame-dried under flowing N_2. This solution was stirred overnight at room temperature, and then refluxed for 4 h. The resulting viscous liquid was diluted with 30−60 mL NMP, and poured into ethanol (250−500 mL). The precipitate was filtered and then dried overnight in a vacuum oven at 40 °C. The dried polymer fibers were then dissolved in CH_2Cl_2 and precipitated in ethanol. The polymer fibers were filtered and then dried overnight in a vacuum oven at 40−55 °C.

SWCNT−Polyimide (2) Nanocomposites. Polyimide **2** (1 g) was dissolved in about 10 mL of DMF/NMP (4:1) and the resulting solution was mixed either with pristine SWCNTs or with the SWCNT/**1** complexes (prepared by the method described earlier in this section) previously dispersed in DMF/NMP (4:1). The final solution was poured into a Petri dish, and heated in a vacuum oven (with high vacuum) at 65 °C overnight. The next day, the temperature was increased to 125 °C for 2 h to completely remove the solvent. The result is a thin flexible film.

3. RESULTS AND DISCUSSION

SWCNT/**1** complexes were prepared by adding purified pristine single-wall carbon nanotubes to a DMF solution of pyrene butanamide **1** as described in the Experimental Section. Compound **1** is designed to enable dispersion of SWCNTs in both organic solvents and polymers and to enhance the SWCNT/polymer interface. The pyrene terminal group in **1** can complex with side walls of SWCNT through $\pi-\pi$ interactions. The amide functionality enables enhanced solubility of the SWCNT/**1** complexes in polar solvents through dipolar interactions and hydrogen bonding. The terminal nadimide group, commonly used as a reactive endcap in high temperature polyimides, will undergo crosslinking with a polyimide matrix at elevated temperatures (59). SWCNT/**1** complexes can be dispersed in DMF in about 10 min or less using either water bath or ultrasonication. These dispersions are stable for days at room temperature and can be used directly in the in situ preparation of polyimide nanocomposites.

SWCNT/**1** complexes were characterized by both spectroscopic and thermal analytical techniques. A comparison of the FT-IR spectra of purified SWCNTs, pyrene butanamide **1**, and the SWCNT/**1** complexes is shown in Figure 1. The FT-IR spectrum of the SWCNT/**1** complexes shows the same carbonyl band at 1704 cm^{-1} as that found in the infrared spectrum of pyrene butanamide **1** (Figure 1c). This confirms that the pyrene butanamide **1** is present on the nanofiller SWCNTs.

SWCNTs electronic transitions can be recorded using UV−vis absorption spectra in solutions or films of the SWCNTs (60–62). These electronic transitions occur between singularities in the density of states of the band structure of the SWCNTs and are known as Van Hove singularity or band (60–63). Figure 2 shows the UV−vis spectra recorded of purified pristine SWNTs and SWNT/**1** complexes in solution. One milligram of either pristine SWCNTs or SWCNT/**1** complexes in 10 mL of *o*-DCB was used. At this low concentration and using *o*-DCB as a solvent, each sample maintains a reasonable dispersion to obtain their spectra. The intensity of the characteristic SWCNTs Van Hove bands of the SWCNT/**1** complexes is lower than that of the pristine SWCNTs. Although some reduction in intensity is expected because of the fact that there is a lesser amount of nanotubes in the complexes (vide infra), this reduction in intensity also suggests that complexation of the

Scheme 2. Synthesis of BPADA/BAPP Polyimide (2)

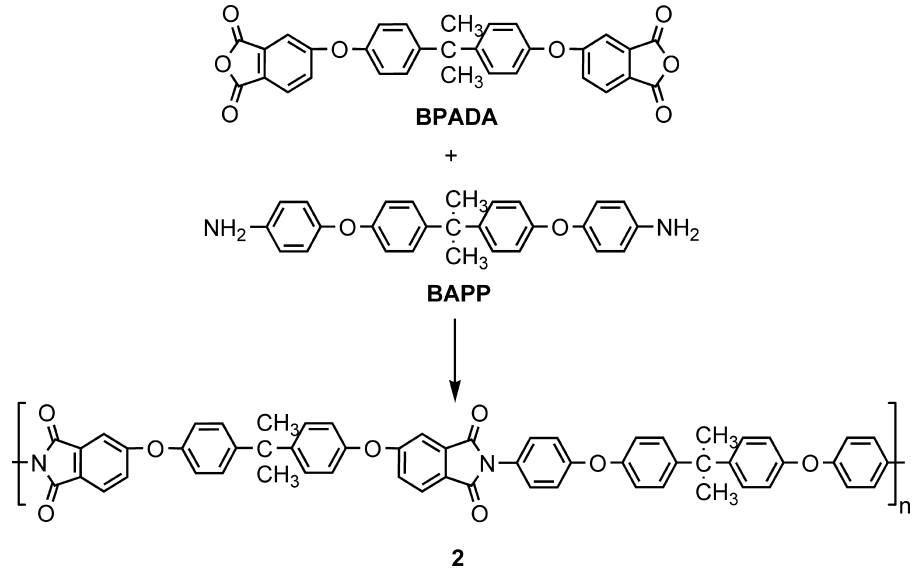

SWCNTs with the pyrene butanamide **1** leads to a perturbation of their π system (63–70).

Thermal gravimetric analysis (TGA) was performed on pristine SWCNTs, SWCNT/**1** complexes and pyrene butanamide **1** under nitrogen. A comparison is given in Figure 3. The thermal analysis for the purified pristine SWCNTs do not exhibit any onset of decomposition, T_d, at temperatures up to 900 °C, the SWCNT/**1** complexes start to degrade at about 225 °C. This T_d is identical to that observed for the pyrene butanamide **1**. As previously shown in the literature, TGA under an inner atmosphere can be use to estimate the degree of functionalization (66). In this case, the residual weight loss obtained for SWCNT/**1** complexes is about 58 wt %. However, because the pyrene butanamide **1** do not decompose completely (leveling off at T_d around 450 °C, and 20 wt %), the residual weight loss between the SWCNT/**1** complexes and pyrene butanamide **1** (i.e., 22 wt %) was substrate to the initial weight loss obtained for the SWCNT/**1** complexes. Thus, the amount of coverage of pyrene butanamide **1** on the nanotubes surface is approximately 36 wt %.

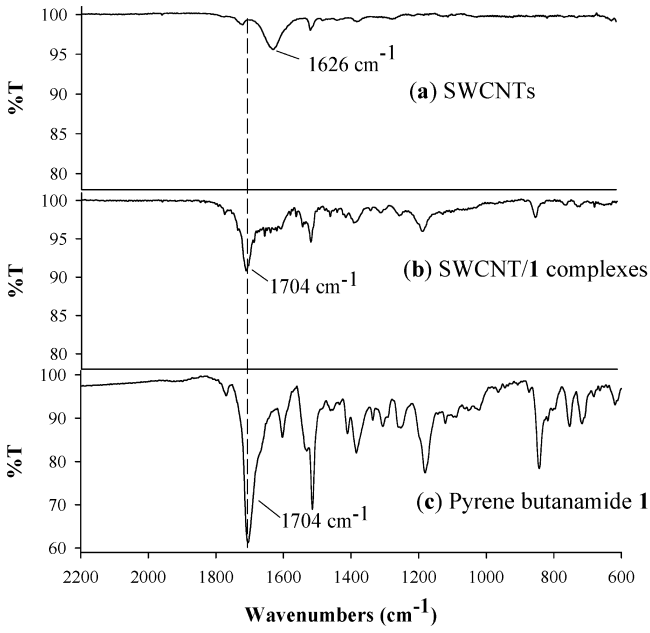

FIGURE 1. FT-IR spectra of (a) SWCNTs, (b) SWCNT/1 complexes, and (c) pyrene butanamide 1.

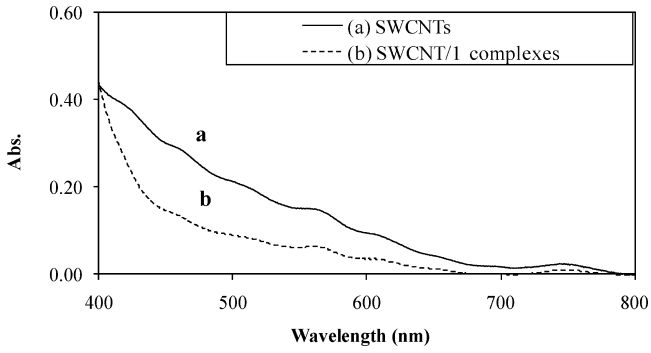

FIGURE 2. UV–vis spectra of (a) SWCNTs and (b) SWCNT/1 complexes.

BPADA/BAPP (**2**) polyimide nanocomposites were prepared with varying amounts of pristine SWCNTs and SWCNT/**1** complexes. The bar chart in Figure 4 shows a comparison of these nanocomposite films as a function of SWCNT loading. Each data entry represents the average

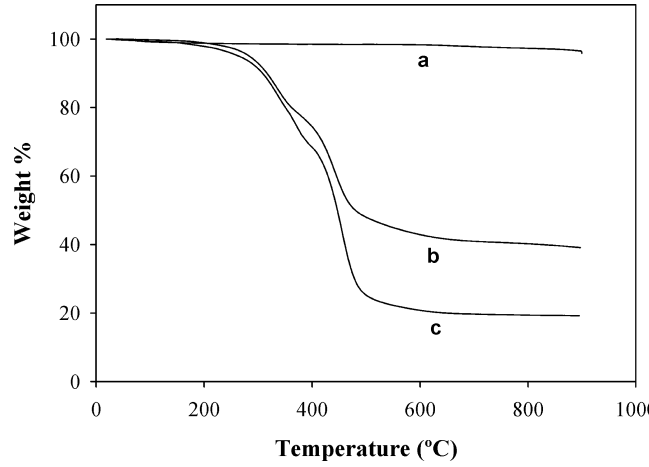

FIGURE 3. TGA (under nitrogen) of (a) pristine SWCNTs, (b) SWCNT/1 complexes, and (c) pyrene butanamide 1.

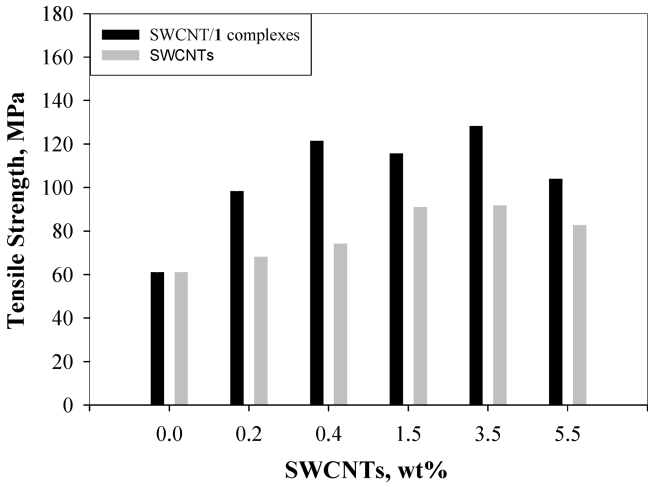

FIGURE 4. Bar chart reporting the effect that occurs by the addition of pristine SWCNTs and SWCNT/1 complexes on the tensile strength of a BPADA/BAPP polyimide film.

value of tensile measurements obtained from testing six nanocomposite film samples (cut from a larger nanocomposite film that had been cast from DMF).

Addition of SWCNTs and SWCNT/**1** complexes enhance the tensile strengths properties of the polyimide films in comparison with the neat polyimide film. Tensile strengths increased with increasing amounts of nanoadditives and tended to level off at between 1.5 and 3.5 wt %. However, at loading levels at or above 5.5 wt %, the nanocomposite films became stiffer and more brittle and the tensile strengths of the nanocomposite films decreased.

The addition of SWCNT/**1** complexes had a larger effect on nanocomposite tensile strength than did the addition of neat SWCNTs. Addition of the 3.5 wt % of SWCNT/**1** increased the tensile strength from 61.35 MPa (neat polyimide) to 128.60 MPa, an improvement of about 109%, compared to a 50% improvement (95 MPa) with the uncomplexed nanotubes (Figure 4).

The greater improvement in the tensile strength of films prepared with SWCNT/**1** complexes is due to reduced formation of SWCNTs agglomerates during the film casting process as well as enhanced interfacial bonding. This behavior is consistent with the reported in the literature (34–55). In addition, the presence of the amide functionality on surface of the SWCNT/**1** complexes also enhances dipole−dipole interactions between the nanotubes and the matrix, thereby leading to a stronger interface and better tensile properties.

Photographs and SEM images of nanocomposite films prepared from pristine SWCNTs and SWCNT/**1** complexes are shown in Figure 5. The SEM images in Figure 5 show that in both cases the present of the SWNTs and SWNTs/**1** complexes in the films. In the photographs, agglomeration of SWCNTs is clearly visible the pristine SWCNTs nanocomposite film (Figure 5a), the nanocomposite film prepared with SWCNT/**1** complexes (Figure 5b) appears more homogeneous with no chunk of agglomeration detected visually. TEM images and discussion of the polyimide nanocomposite on both cases can be found in the Supporting Information.

The storage modulus of the polyimide films also increased with addition of both neat SWCNT and SWCNT/**1** complex. Dynamic mechanical analysis (DMA) plots measured on nanocomposite films of various loading levels of SWCNT or SWCNT/**1** complexes as well as the neat polyimide film are shown in Figure 6 (plots obtained from one representative sample of the polyimide nanocomposite films). The storage modulus of the neat polyimide film at 30 °C was 142 MPa. Addition of 1.5, 3.5, or 5.5 wt % SWCNTs increased the storage modulus to 351, 1201, and 2272 (60 °C) MPa, respectively (Figure 6a). Significantly higher storage moduli were observed in nanocomposite films made with SWCNT/**1** complexes (Figure 6b). At loading levels of 1.5, 3.5, and 5.5 wt % of SWCNT/**1** complexes, the storage moduli of the resulting nanocomposite films were 436, 2617, and 3025 MPa, respectively.

The effect of addition of SWCNTs and SWCNT/**1** complexes on the temperature at 5% weight loss in the TGA ($T_{5\%}$), the glass transition temperatures (T_g), and the coefficient of thermal expansion (CTE) are given in Table 1 as a function of loading level. The glass transition temperature of the polyimide films increased with increasing loading levels of both additives. However, this increase was more dramatic with addition of SWCNT/**1** complexes. Addition of both nanoscale additives also improved the thermal-oxidative stability of the polyimide films as evidenced by increases in $T_{5\%}$, the temperature at 5% weight loss in the TGA. For T_g and $T_{5\%}$, better improvements were observed with addition of the SWCNT/**1** complexes than pristine SWCNTs at the same loading levels. At 5.5 wt %, the T_g was enhanced by 28 °C compared to 16 °C (SWCNT/**1** complexes vs pristine SWCNTs), and $T_{5\%}$ increased by 122 °C compared to 101 °C. While addition of pristine SWCNTs did lead to a slight reduction in the CTE of the film, addition of SWCNT/**1** complexes had little or no effect. We found a reduction of CTE up to 24% with the present of pristine SWCNTs. However, in the case of SWCNT/**1** complexes, a slightly increase up to 5% was obtained. This mismatch effect is particularly interesting because previous report shows that the CTE with either pristine SWCNTs or functionalized SWCNTs in polymer resin has the tendency to decrease (71–73).

The materials of the structures play an important role in the CTE magnitude. For single-phase materials, usually shows a large CTE because of a low bonding energy that occurs as the temperature increases. On the other hand, for multiphase material, the CTE depend not only on the phases but also on the interaction of each component which with a weak interface bonding mostly result in the reduction on the CTE (73). In our case, using SWCNT/**1** complexes did not show a reduction in CTE. This behavior may be explained as a consequence of effective interface interactions between the SWCNTs, pyrene butanamide **1** and the polyimide.

Volume (DC) resistivities were measured on nanocomposite films prepared with various loading levels of SWCNT and SWCNT/**1** complexes. A constant voltage two-point probe technique was used for these measurements at 100

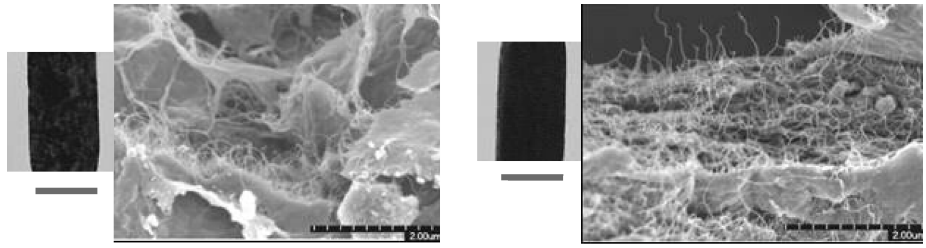

a b

FIGURE 5. Photographs (9 mm) and SEM images of polyimide nanocomposite films prepared from (a) pristine SWCNTs, and (b) SWCNT/1 complexes.

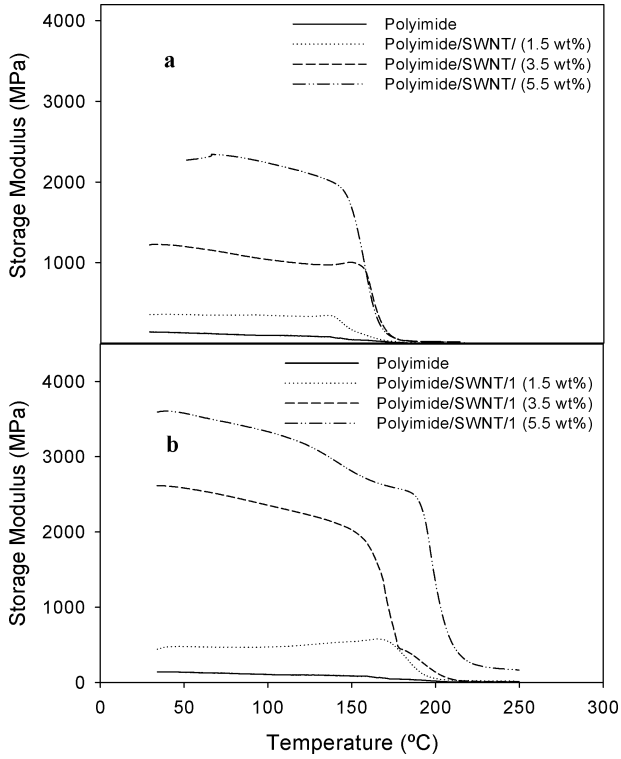

FIGURE 6. DMA plots of polyimide nanocomposite films: (a) polyimide/SWCNT, (b) polyimide/SWCNT/1.

Table 1. Temperature at 5% Weight Loss in the TGA, $T_{5\%}$, Glass Transition Temperatures, T_g, and the Coefficient of Thermal Expansion, CTE, of SWCNT and SWCNT/1 Nanocomposites

additive	$T_{5\%}$[a] (°C)	T_g[b] (°C)	CTE[c] (ppm/°C)
no additive	388	169	21/60
1.5 wt % SWCNTs	408	168	20/60
3.5 wt % SWCNTs	410	188	18/60
5.5 wt % SWCNTs	489	185	16/60
1.5 wt % SWCNT/**1**	486	184	21/60
3.5 wt % SWCNT/**1**	481	188	22/60
5.5 wt % SWCNT/**1**	510	197	22/60

[a] $T_{5\%}$, measured by TGA in air at a heating rate of 10 °C/min. [b] Measured by DMA in N_2 at a heating rate of 10 °C/min. [c] CTE measured by TMA in N_2 at a heating rate of 10 °C/min.

V applied voltage and currents ranging from 0.3 to 70 μA. The results of these measurements are displayed in Tables 2 and 3 (in form of volume conduction) for films made from SWCNTs and SWCNT/**1** complexes, respectively. Resistivities of films having loading levels below 0.2 weight percent

Table 2. Conductivity of SWCNT Nanocomposites

wt % SWCNTs	thickness (mm)	width (cm)	length (cm)	voltage (V)	current (A)	conductivity (S cm^{-1})
1.00	2.5	0.75	3.8	100	1.00×10^{-13}	7.69×10^{-13}
5.00	3.5	0.85	3.8	100	3.00×10^{-12}	1.51×10^{-11}
9.00	5.5	0.90	3.9	100	1.02×10^{-5}	3.12×10^{-5}

Table 3. Conductivity of SWCNT/1 Nanocomposites

wt % SWCNT/**1**	thickness (mm)	width (cm)	length (cm)	voltage (V)	current (A)	conductivity (S cm^{-1})
1.50	3.5	0.90	3	100	1.26×10^{-9}	4.76×10^{-9}
3.50	3.5	0.95	3	100	1.23×10^{-8}	4.34×10^{-8}
5.50	3.5	0.88	3.3	100	3.69×10^{-6}	1.56×10^{-5}
9.00	3	0.80	4.2	100	2.07×10^{-5}	1.42×10^{-4}

exceeded the detection limits of the instrument used (1.3×10^{12} ohm-cm) and could not be measured. Plots of the conductivities of the nanocomposite films as function of loading levels are shown in Figure 7 for both SWCNTs and SWCNT/**1** complexes.

The electrical conductivity of the nanocomposite films increases with the addition of SWCNTs. The conductivity of SWCNT/**1** nanocomposite at 5.5 wt % (1.56×10^{-5} S cm^{-1}) is considerable higher than that of the nanocomposite film prepared with pristine SWCNTs (5.0 wt %, 1.51×10^{-11} S cm^{-1}). This is likely a consequence of the efficient intermolecular interactions between SWCNTs due to the improved dispersions obtained by using SWCNT/**1** complexes. Similar reductions in volume resistivities (i.e., increase in volume conductivities) of polyimide films with the addition of nanotube complexes have been reported in the literature. For

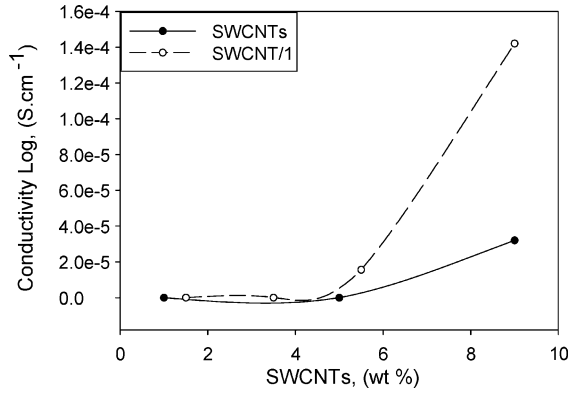

FIGURE 7. Effect of addition of pristine SWCNTs and SWCNT/1 complexes on the electrical resistivity of BPADA/BAPP polyimide films.

example, Delozier and co-workers (74) report that addition of 1.6 wt % SWCNTs complexed with a bis(pyrillium) salt-based ionomer reduced the volume resistivity of a CP-2 polyimide film from >1 $\times$ 10^{12} S cm to 3.0 $\times$ 10^{8} S cm (3.3 $\times$ 10^{-9} S cm^{-1}). By comparison, the volume resistivity of polyimide **2** containing 1.5 wt % SWCNT/**1** was measured at 2.0 $\times$ 10^{8} S cm (5.0 $\times$ 10^{-9} S cm^{-1}). The higher electrical conductivity obtained for SWCNT/**1** nanocomposite at 5.5 wt % is an effect of having fewer bundles of ropes of SWCNTs present in the nanocomposite and permitting in this way a more efficient heat transfer through out the polyimide film.

4. CONCLUSIONS

We report the preparation and characterization of noncovalent functionalization of SWCNTs with a nadic terminated pyrene butanamide **1**, and compares the effects of pristine SWCNTs and SWCNT/**1** complexes on the mechanical, thermal and electrical properties of polyimide. Although in the literature we can find the use of aromatics molecules to functionalized SWCNTs, to the best of our knowledge there is no evidence of work reported on the use of this aromatics noncovalent functionalized SWCNTs to prepare polyimide nanocomposites and studies their mechanical, electrical, and thermal properties. We found that polyimide films prepared with the SWCNT/**1** complexes showed higher tensile strengths and storage moduli than that of the neat polyimide film and polyimide nanocomposite films prepared with pristine SWCNTs at the same loading levels. These films also had higher glass transition temperatures and better high-temperature stability than both the neat polyimide films and corresponding nanocomposite films prepared with pristine SWCNTs. In addition, DC volume conductivities increased significantly with addition of these complexes and were higher than nanocomposite films prepared with uncomplexed SWCNTs. These materials are of interest because they could be suitable for use as multifunctional materials in applications where the combination of good mechanical properties and electrical conductivity are required.

Acknowledgment. This work was supported by Fundamental Aeronautics Program, Subsonic Fixed Wing Project.

Supporting Information Available: Thermal gravimetric analysis (TGA) plots and transmission electron microscope (TEM) studies (PDF). This material is available free of charge via the Internet at http://pubs.acs.org.

REFERENCES AND NOTES

(1) Ruoff, R. S.; Lorents, D. C. *Carbon* **1995**, *33*, 135–140.
(2) Hamada, N.; Sawada, S.; Oshiyama, A. *Phys. Rev. Lett.* **1992**, *68*, 1579–1581.
(3) Yakobson, B. I.; Avouris, P. In *Carbon Nanotubes: Synthesis, Structure, Properties, and Applications*; Topics in Applied Physics; Springer-Verlag: Heidelberg, Germany, 2000; Vol. 80, p 299.
(4) Robertson, D. H.; Brenner, D. W.; Mintmire, J. W. *Phys. Rev. B* **1992**, *45*, 12592–12592.
(5) Yakobson, B. I.; Brabec, C. J.; Bernholc, J. *Phys. Rev. Lett.* **1996**, *76*, 2511–2514.
(6) Cornwell, C. F.; Wille, L. T. *Solid State Commun.* **1997**, *101*, 555–558.
(7) Hernández, E.; Goze, C.; Bernier, P.; Rubio, A. *Phys. Rev. Lett.* 199880, 4502–4505.
(8) Dekker, C. *Phys. Today* **1999**, 22–28.
(9) Krishnan, A.; Dujardin, E.; Ebbesen, T. W.; Yianilos, P. N.; Treacy, M. M. J. *Phys. Rev. B* **1998**, *58*, 14013–14019.
(10) Salvetat, J.-P.; Bonard, J.-M.; Thomson, N. H.; Kulik, A. J.; Forró, L.; Benoit, W.; Zuppiroli, L. *Appl. Phys. A: Mater. Sci. Process.* **1999**, *69*, 255–260.
(11) Ajayan, P. M. *Chem. Rev.* **1999**, *99*, 1787–1800.
(12) Ye, Y.; Ahn, C. C.; Witham, C.; Fultz; Liu, J.; Rinzler, A. G.; Colbert, D.; Smith, K. A.; Smalley, R. E. *Appl. Phys. Lett.* **1999**, *74*, 2307–2309.
(13) Haggenmueller, R.; Gommans, H. H.; Rinzler, A. G.; Fischer, J. E.; Winey, K. I. *Chem. Phys. Lett.* **2000**, *330*, 219–225.
(14) Quian, D.; Dickey, E. C.; Andrews, R.; Rantell, T. *Appl. Phys. Lett.* **2000**, *76*, 2868–2870.
(15) Zhang, X.; Liu, T.; Sreekumar, T. V.; Kumar, S.; Moore, V. C.; Hauge, R. H.; Smalley, R. E. *Nano Lett.* **2003**, *3*, 1285–1288.
(16) Shaffer, M. S. P.; Windle, A. H. *Adv. Mater.* **1999**, *11*, 937.
(17) Bower, C.; Rosen, R.; Jin, L.; Han, J.; Zhou, O. *Appl. Phys. Lett.* **1999**, *74*, 3317–3319.
(18) Jin, L.; Bower, C.; Zhou, O. *Appl. Phys. Lett.* **1998**, *73*, 1197–1199.
(19) Sandler, J.; Shaffer, M. S. P.; Prasse, T.; Bauhofer, W.; Schulte, K.; Windler, A. H. *Polymer* **1999**, *40*, 5967–5671.
(20) Sandler, J. K. W.; Kirl, J. E.; Kinloch, I. A.; Shaffer, M. S. P.; Windle, A. H. *Polymer* **2003**, *44*, 5893–5899.
(21) Ajayan, P. M.; Stephan, O.; Colliex, C.; Trauth, D. *Science* **1994**, *265*, 1212.
(22) Schadler, L. S.; Giannaris, S. C.; Ajayan, P. M. *Appl. Phys. Lett.* **1998**, *73*, 3842–3844.
(23) Lourie, O.; Wagner, H. D. *Appl. Phys. Lett.* **1998**, *73*, 3527–3529.
(24) Wagner, H. D.; Lourie, O.; Feldman, Y.; Tenne, R. *Appl. Phys. Lett.* **1998**, *72*, 188–190.
(25) Sun, Y. P.; Huang, A.; Lin, Y.; Fu, K.; Kitaygorodskiy, A.; Riddle, L. A.; Yu, Y. J.; Carroll, D. L. *Chem. Mater.* **2001**, *13*, 2864–2869.
(26) Chen, J.; Hamon, M. A.; Hu, H.; Chen, Y.; Rao, A. M.; Eklund, P. C.; Haddon, R. C. *Science* **1998**, *282*, 95–98.
(27) Zeng, H. L.; Gao, C.; Yan, D. Y. *Adv. Funct. Mater.* **2006**, *16*, 812–818.
(28) Shen, J. F.; Huang, W. S.; Wu, L. P.; Hu, Y. Z.; Ye, M. X. *Compos. Sci. Technol.* **2007**, *67*, 3041–3050.
(29) Ma, P. C.; Kim, J. K.; Tang, B. Z. *Compos. Sci. Technol.* **2007**, *67*, 2965–2972.
(30) Wang, M.; Pramoda, K. P.; Goh, S. H. *Carbon* **2006**, *44*, 613–617.
(31) Tagmatarchis, N.; Prato, M. *J. Mater. Chem.* **2004**, *14*, 437–439.
(32) Dyke, C. A.; Tour, J. M. *J. Phys. Chem. A* **2005**, *108*, 11151–11159.
(33) Khabashesku, V. N.; Billups, W. E.; Margrave, J. L. *Acc. Chem. Res.* **2002**, *35*, 1087–1095.
(34) Chen, J.; Ramasubramaniam, R.; Xue, C. H.; Liu, H. Y. *Adv. Funct. Mater.* **2006**, *16*, 114–119.
(35) Zorbas, V.; Acevedo, A. O.; Dalton, A. B.; Yoshida, M. M.; Dieckmann, G. R.; Draper, R. K.; Baughman, R. H.; Yacaman, M. J.; Musselman, I. H. *J. Am. Chem. Soc.* **2004**, *126*, 7222–7227.
(36) Yang, Z.; Chen, X. H.; Pu, Y. X.; Zhou, L. P.; Chen, C. S.; Li, W. H.; Xu, L. S.; Yi, B.; Wang, Y. G. *Polym. Adv. Technol.* **2007**, *18*, 458–462.
(37) Kim, K. K.; Yoon, S. M.; Choi, J. Y.; Lee, J. H.; Kim, B. K.; Kim, J. M.; Lee, J. H.; Paik, U.; Park, M. H.; Yang, C. W.; An, K. H.; Chung, Y. S.; Lee, Y. H. *Adv. Funct. Mater.* **2007**, *17*, 1775–1783.
(38) Chen, J.; Liu, H. Y.; Weimer, W. A.; Halls, M. D.; Waldeck, D. H.; Walker, G. *J. Am. Chem. Soc.* **2002**, *124*, 9034–9035.
(39) Chatterjee, T.; Yurekli, K.; Hadjiev, V. G.; Krishnamoor, R. *Adv. Funct. Mater.* **2005**, *15*, 1832–1838.
(40) Richard, C.; Balavoine, F.; Schulta, P.; Ebbesen, T. W.; Mioskowski, C. *Science* **2003**, *300*, 775–778.
(41) Du, F.; Fischer, J. E.; Winey, K. I. *J. Poly. Sci. Part B: Poly. Phys.* **2003**, *41*, 3333–3338.
(42) Zhu, J.; Kim, J. D.; Peng, H.; Margrave, J. L.; Khabashesku, V. N.; Barrera, E. V. *Nano. Lett.* **2003**, *3*, 1107–1113.
(43) Mitchell, C. A.; Bahr, J. L.; Arepalli, S.; Tour, J. M.; Krishnamoorti, R. *Macromolecules* **2002**, *35*, 8825–8830.
(44) Furtado, C. A.; Kim, U. J.; Gutierrez, H. R.; Pan, L.; Dickey, E. C.; Eklund, P. C. *J. Am. Chem. Soc.* **2004**, *126*, 6095–6105.
(45) Zhang, X.; Liu, T.; Sreekumar, T. V.; Kumar, S.; Moore, V. C.; Hauge, R. H.; Smalley, R. E. *Nano Lett.* **2003**, *3*, 1285–1288.
(46) Hu, C.-Y.; Xu, Y.-J.; Duo, S.-W.; Zhang, R.-F.; Li, M.-S. *J. Chinese Chem. Soc.* **2009**, *56*, 234–239.

(47) Liu, X.; Chan-Park, M. B. *J. Appl. Polym. Sci.* **2009**, *114*, 3414–3419.
(48) Chen, R. J.; Zhang, Y.; Wang, D.; Dai, H. *J. Am. Chem. Soc.* **2001**, *123*, 3838–3839.
(49) Lauffer, P.; Jung, A.; Graupner, R.; Hirsch, A.; Ley, L. *Phys. Stat. Sol. (b)* **2006**, *243*, 3213–3216.
(50) Hu, C.; Chen, Z.; Shen, A.; Shen, X.; Li, J.; Hu, S. *Carbon* **2006**, *44*, 428–434.
(51) Nakayama-Ratchford, N.; Bangsaruntip, S.; Sun, X.; Welsher, K.; Dai, H. *J. Am. Chem. Soc.* **2007**, *129*, 2448–2449.
(52) Ferreira, O. P.; Otubo, L.; Aguiar, A. L.; Silva, J. J. A.; Filho, J. M.; Filho, A. G. S.; Fagan, S. B.; Alves, O. L. *J. Nanopart. Res.* **2009**, *11*, 2163–2170.
(53) Tasis, D.; Mikroyannidis, J.; Karoutsos, V.; Galiotis, C.; Papagelis, K. *Nanotechnology* **2009**, *20*, 1–7.
(54) Park, S.; Huh, J. O.; Kim, N. G.; Kang, S. M.; Lee, K.-B.; Hong, S. P.; Do, Y.; Choi, I. S. *Carbon* **2008**, *46*, 706–720.
(55) Lemek, T.; Mazurkiewicz, J.; Stobinski, L.; Lin, H. M.; Tomasik, P. *J. Nanosci. Nanotechnol.* **2007**, *7*, 3081–3088.
(56) Nikolaev, P.; Bronikowski, M. J.; Bradley, R. K.; Rohmund, F.; Colbert, D. T.; Smith, K. A.; Smalley, R. E. *Chem. Phys. Lett.* **1999**, *313*, 91–97.
(57) Lebrón-Colón, M. Purification, Characterization and Functionalization of Single-Wall Carbon Nanotubes for Aerospace Applications. Thesis/Dissertation, Clark Atlanta University, Atlanta, 2004.
(58) Rosario-Castro, B. I.; Contés, E. J.; Lebrón-Colón, M.; Meador, M. A.; Sánchez-Pomales, G.; Cabrera, C. R. *Mater. Charact.* **2009**, *60*, 1442–1453.
(59) Chuang, K. C.; Scheiman, D. A.; Fu, J.; Crawford, M. *J. Polym. Sci., A: Polym. Chem.* **1999**, *37*, 2559–2567.
(60) Hamon, M. A.; Itkis, M. E.; Niyogi, S.; Alvaraez, T.; Kuper, C.; Menon, M.; Haddon, R. C. *J. Am. Chem. Soc.* **2001**, *123*, 11292–11293.
(61) Odom, T. W.; Hiang, J.-L.; Kim, P.; Lieber, C. M. *J. Phys. Chem. B* **2000**, *104*, 2794–2809.
(62) Kataura, H.; Kumazawa, Y.; Maniwa, Y.; Umezu, I.; Suzuki, S.; Ohtsuka, Y.; Achiba, Y. *Synth. Met.* **1999**, *103*, 2555–2558.
(63) Chen, J.; Hannon, M. A.; Hu, H.; Chen, Y.; Rao, A. M.; Ecklund, P.; Haddon, R. C. *Science* **1998**, *282*, 95–98.
(64) Riggs, J. E.; Guo, Z.; Carroll, D. L.; Sun, Y. P. *J. Am. Chem. Soc.* **2000**, *122*, 5879–5880.
(65) Boul, P. J.; Liu, J.; Mickelson, E. T.; Huffman, C. B.; Ericson, L. M.; Chiang, I. W.; Smith, K. A.; Colbert, D. T.; Hauge, R. H.; Margrave, J. L.; Smalley, R. E. *Chem. Phys. Lett.* **1999**, *310*, 367–372.
(66) Bahr, J. L.; Yang, J.; Kosynkin, D. V.; Bronikowski, M. J.; Smalley, R. E.; Tour, J. M. *J. Am. Chem. Soc.* **2001**, *123*, 6536–6542.
(67) Bahr, J. L.; Mickelson, I. T.; Bronikowski, M. J.; Smalley, R. E.; Tour, J. M. *Chem. Commun.* **2001**, *2*, 193–194.
(68) Sun, Y.; Wilson, S. R.; Schuster, D. I. *J. Am. Chem. Soc.* **2001**, *123*, 5348–5349.
(69) Georgakilas, V.; Kordatos, K.; Prato, M.; Guldi, D. M.; Holzinger, M.; Hirsch, A. *J. Am. Chem. Soc.* **2002**, *124*, 760–761.
(70) Bandyopadhyaya, R.; Nativ-Roth, E.; Regev, O.; Yerushalmi-Rozen, R. *Nano Lett.* **2002**, *2*, 25–28.
(71) Wei, C.; Srivastava, D.; Cho, K. *Nano Lett.* **2002**, *2*, 647–650.
(72) Xu, Y.; Ray, G.; Abdel-Magid, B. *Composites, Part A* **2006**, *37*, 114–121.
(73) Wang, S.; Liang, Z.; Gonnet, P.; Liao, Y.-H.; Wang, B.; Chuck, Z. *Adv. Funct. Mater.* **2007**, *17*, 87–92.
(74) Delozier, D. M.; Tigelaar, D. M.; Watson, K. A.; Smith, J. G., Jr.; Kelin, D. J.; Lillehei, P. T.; Connell, J. W. *Polymer* **2005**, *46*, 2506–2521.

AM900682S